

Supplementary Information

Eugene Tan^{1*}, Shannon D. Algar¹, Débora Corrêa², Thomas Stemler¹ and Michael Small^{1,3}

¹The Complex Systems Group, Department of Mathematics & Statistics, The University of Western Australia, Crawley, Australia, 6009.

²Department of Computer Science & Software Engineering, The University of Western Australia, Crawley, Australia, 6009.

³Mineral Resources, CSIRO, Kensington, Australia, 6151.

*Corresponding author(s). E-mail(s): eugene.tan@uwa.edu.au;

Contributing authors: shannon.algar@uwa.edu.au;

debora.correa@uwa.edu.au; thomas.stemler@uwa.edu.au;

michael.small@uwa.edu.au;

Supplementary Note 1: VF Detection with Comparison Methods

001
002
003
004
005
006
007
008
009
010
011
012
013
014
015
016
017
018
019
020
021
022
023
024
025
026
027
028
029
030
031
032
033
034
035
036
037
038
039
040
041
042
043
044
045
046

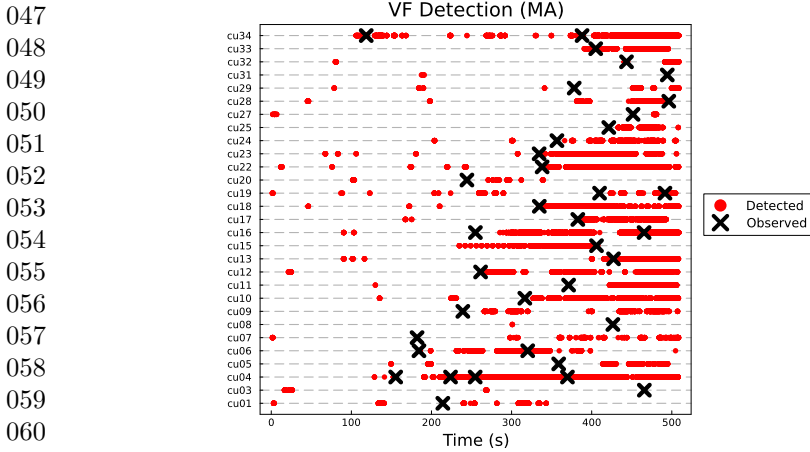
2 *Supplementary Information*

Fig. S1 VF detection results using the moving average as the score for change point detection. Annotated onsets for VF are given black crosses, and flagged detection of VF is given by a red dot. The onset of VF is characterised by a persistent detection result (red).

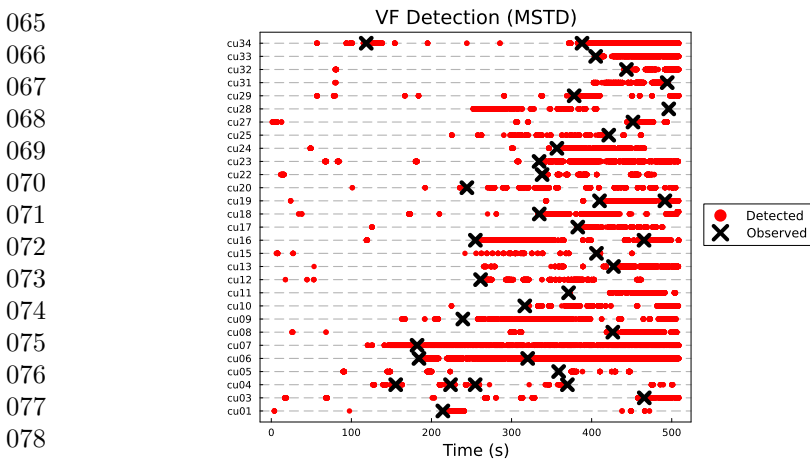


Fig. S2 VF detection results using the moving standard deviation as the score for change point detection. Annotated onsets for VF are given black crosses, and flagged detection of VF is given by a red dot. The onset of VF is characterised by a persistent detection result (red).

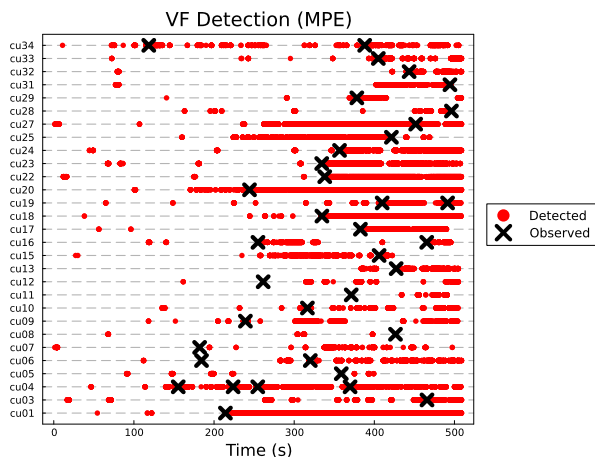


Fig. S3 VF detection results using the moving permutation entropy as the score for change point detection. Annotated onsets for VF are given black crosses, and flagged detection of VF is given by a red dot. The onset of VF is characterised by a persistent detection result (red).

Supplementary Note 2: Phase Coherence vs. Non-Phase Coherence Detection

Chaotic oscillators such as the Rössler system are distinct from periodic systems in that they do not exhibit an exact frequency [1]. Observation of the power spectrum of chaotic signals reveals activations across the whole band of considered frequencies. Phase coherence (PC) within a chaotic oscillator is characterised by the presence of a well defined peak on the power spectrum. An equivalent condition is that the phase of the signal changes monotonically where the phase can be approximated from the signal using a Hilbert transform [2]. This often corresponds to trajectories in phase space that rotate along a collection of orbits around some central point [1]. Parallel trajectories on these orbits have phases that are similar throughout the whole period of rotation. In contrast, non-phase coherent (NPC) systems do not have a clearly defined phase relationship over time.

The Rössler chaotic oscillator is one that exhibits both PC and NPC dynamics at different bifurcation values (see Fig. S5) [2] with system equations given by

$$\begin{aligned}\dot{x} &= -y - z, \\ \dot{y} &= x + \alpha y, \\ \dot{z} &= z(x - c),\end{aligned}$$

4 *Supplementary Information*

139
 140
 141
 142
 143
 144
 145
 146
 147
 148
 149
 150
 151
 152
 153
 154
 155
 156
 157
 158
 159
 160
 161
 162
 163
 164
 165
 166
 167
 168
 169
 170
 171
 172
 173
 174
 175
 176
 177
 178
 179
 180
 181
 182
 183
 184

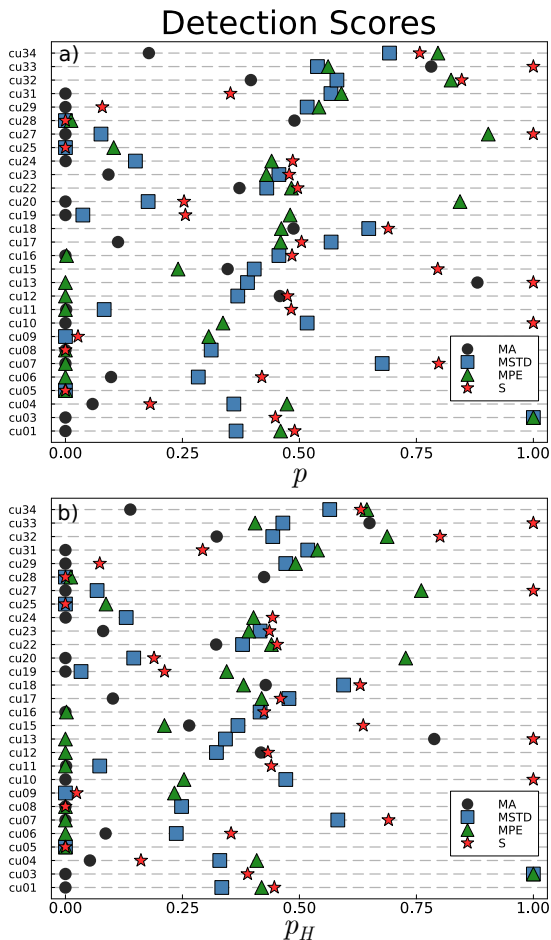


Fig. S4 Detection performance scores for each patient compared across four methods: moving average (MA), moving standard deviation (MSTD), moving permutation entropy (MPE), and surprise (S). **(a)** raw performance score p and **(b)** performance score adjusted for successive detections.

where $b = 0.4$ and $c = 8.5$. The phase coherence of the system can be controlled by the parameter $\alpha = 0.165$ and $\alpha = 0.265$ corresponding to the PC and NPC regimes respectively. This results in two similar attractors with structurally different features. From Figure S5 the PC attractor is close to a subset of the NPC regime. Hence, the attractor network approach that quantifies attractor changes would be able to detect changes from PC to NPC but not the reverse. This feature was used to test the attractor network approach in detecting changes in attractor structure in phase space.

Here, the change point detection task is to identify when the signal changes between the PC and NPC regime. To do this, an attractor network is trained on data generated from a Rössler system operating in the PC regime. An additional shorter length of training data of length 20000 was used to get

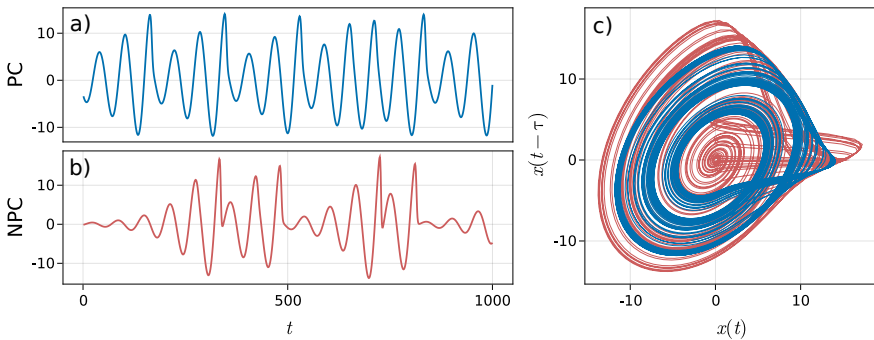
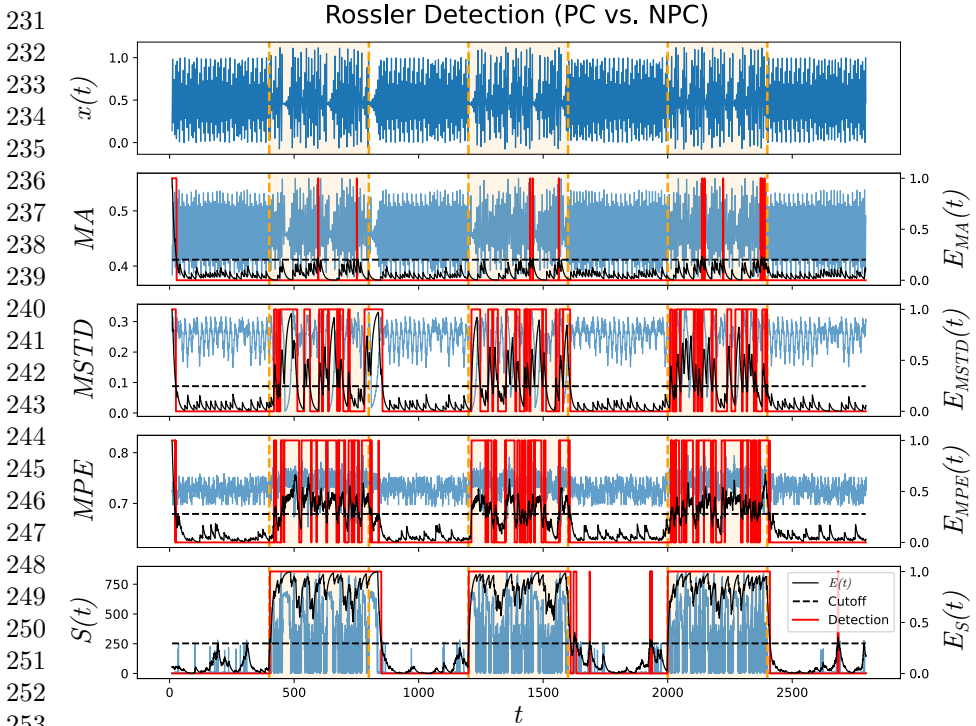


Fig. S5 Time series of the Rössler system operating in the (a) PC ($\alpha = 0.165$) (blue) and (b) NPC ($\alpha = 0.265$) (red) regime. (c) The corresponding phase space reconstruction where the attractor for the PC system (blue) is almost a subset of the NPC attractor (red).

the 95% cutoff value for $S(t)$ operating on the original system. The test data consisted of the simulated oscillator with a modulating bifurcation value α switching between the PC $\alpha = 0.165$ and NPC $\alpha = 0.265$ regimes every 2000 steps. The resulting $S(t)$ was used to evaluate $E(t)$ and determine transition points.

The results revealed that the attractor network method performed equally well if not better than other simpler metrics (moving statistics, permutation entropy) in providing distinct cutoffs for the change points transitions between PC and NPC (see Fig. S6). However, we find that the converse problem of detecting PC transitions using attractor networks trained on NPC was not successful, whereas simpler metrics performed consistently. This difference in performance can be attributed to the fact that the PC Rössler attractor is spatially almost a subset of the NPC attractor (see Fig. S5) when discretised with respect to some selected resolution ϵ . Whilst there exists differences between the state space distributions of both attractors, $S(t)$ aims to capture the surprise of transition at a given point in time. Thus, such a method would be limited to the resolution governed by δ and ϵ as defined in the Methods section.

185
186
187
188
189
190
191
192
193
194
195
196
197
198
199
200
201
202
203
204
205
206
207
208
209
210
211
212
213
214
215
216
217
218
219
220
221
222
223
224
225
226
227
228
229
230



254 **Fig. S6** Results of all change point algorithms for detecting transitions between NPC and
 255 PC Rössler time series. From the top to bottom: Original time series, moving average, moving
 256 standard deviation statistic, moving permutation entropy, and surprise scores $S(t)$. Sliding
 257 window lengths of 100 steps were used for calculating moving averages. Detections (red) are
 258 made based on the exponential smoothed quantity $E(t)$ with respect to a set cutoff E^* . Real
 259 change points are given by vertical orange lines. All methods except the moving average
 260 are able to detect change points. However, only the surprise score produces a persistent
 classification of observations as abnormal.

261 **Supplementary Note 3: Quantifying Gradual** 262 **Transitions**

264 Contrasting with the detection of abrupt changes in the time series, the attractor
 265 network approach was used to see if the surprise metric $S(t)$ could be
 266 used to quantify gradual changes in a system. To test this, we analyse the
 267 Chua dynamical system that is known to contain two disjoint scroll-shaped
 268 attractors,

$$\begin{aligned}
 270 \quad \dot{x} &= -(y - x + z), \\
 271 \quad \dot{y} &= -\alpha(x - y - f(y)), \\
 272 \quad \dot{z} &= \beta x + \gamma z, \\
 273 \quad f(y) &= ay^3 + by,
 \end{aligned}$$

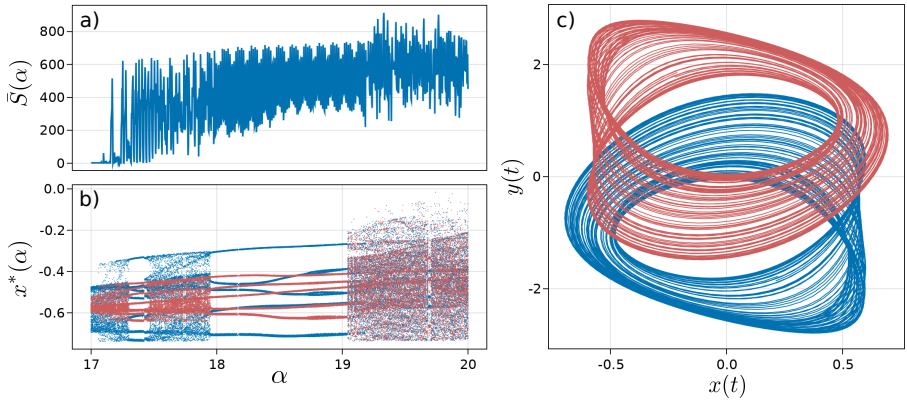


Fig. S7 (a) The calculated average surprise for each 50 step window corresponding to a given value of α with (b) containing the corresponding bifurcation diagram of the system. Blue and red represent the two disjoint scroll attractors which eventually merge at $\alpha \approx 19.05$. (c) The two disjoint scrolls attractors corresponding to the same bifurcation diagram at $\alpha = 17$.

where $(\beta, \gamma, a, b) = (53.612186, -0.75087096, 0.03755, -0.84154)$. For increasing values of $\alpha \in (17, 20)$, the system undergoes a gradual transition from the single scroll to double scroll regime [3]. During the transition, two disjoint scrolls in the Chua attractor gradually merge and undergo a crisis resulting in a single double scroll attractor. Input data from the single scroll Chua system ($\alpha = 17$) with the $dt = 0.1$ and 25000 time steps was used to construct the attractor network. To simulate the transition, the same Chua system was integrated in 1000 segments of 50 timesteps with each segment corresponding to a slight increase in α in the interval $[17, 20]$. The endpoint of each segment is fed as initial conditions for the integration of the next interval to ensure continuity in the time series. Finally, the first component of the test time series is delay embedded and used for calculating $S(t)$.

The resulting profile showing average surprise for each window $\bar{S}(\alpha)$ was found to correspond closely with the various regions in the bifurcation diagram (see Fig. S7). In the single scroll regime with two separate attractors ($\alpha \approx [17, 17.95]$), $\bar{S}(\alpha)$ shows relatively consistent volatile behaviour. The final double scroll regime $\alpha \approx [19.05, 20]$ is also reflected in more disordered and larger amplitude variations. We also note that the periodic regimes ($\alpha \approx [17.3, 17.4] \cup [17.95, 19.05]$) are also tracked well where $\bar{S}(\alpha)$ displays a consistent pseudoperiodic behaviour. Additionally, $\bar{S}(\alpha)$ shows a positive correlation with increasing deviation from the original trained value of $\alpha = 17$. The relatively gradual increase in surprise with increasing perturbation of the bifurcation parameter suggests that the attractor network may be sensitive in measuring the magnitude of change in a given system.

277
278
279
280
281
282
283
284
285
286
287
288
289
290
291
292
293
294
295
296
297
298
299
300
301
302
303
304
305
306
307
308
309
310
311
312
313
314
315
316
317
318
319
320
321
322

323
 324
 325
 326
 327
 328
 329
 330
 331
 332
 333
 334
 335
 336
 337
 338
 339
 340
 341
 342
 343
 344
 345
 346
 347
 348
 349
 350
 351
 352
 353
 354
 355
 356
 357
 358
 359
 360
 361
 362
 363
 364
 365
 366
 367
 368

Supplementary Note 4: Nonlinear Change Point Detection

In this section, we provide additional comparisons between the attractor network approach and two nonlinear time series analysis methods from recurrence quantification analysis. Recurrence quantification analysis is a method that aims to track spatial recurrences of a given trajectory in phase space [4]. Given a multivariate time series $\vec{x}(t) \in \mathbb{R}^m$ of length L , a recurrence matrix R is a $L \times L$ square matrix with entries given by

$$R_{ij} = \begin{cases} 1 & , \|\vec{x}(i) - \vec{x}(j)\| < \epsilon \\ 0 & , \text{otherwise} \end{cases}, \quad (\text{S1})$$

where ϵ is a size scale parameter typically selected such that a proportion r of the entries in L are non-zero. The constant r is commonly termed the recurrence rate.

Broadly speaking, a dynamical system's trajectories may be partially represented by the observed recurrences of its trajectories. Recurrence quantification analysis (RQA) aims to identify measures and properties from R for the purpose of time series analysis. In the context of change point detection, we compare the attractor network approach with two recent RQA-based methods: quadrant scan (QS) and modularity scan (MOD). For the interested reader, we refer to the work by [5] and [6] for further detail on these methods.

We employ a sliding window approach of length 100 and calculate both QS and MOD measures alongside moving average, moving standard deviation, permutation entropy and surprise for change point detection in two cases: (1) Chua AAFS and (2) Rössler PC vs. NPC. The results are provided in Figures S8 and S9.

The recurrence plot measures, QS and MOD, performed similarly and were able to detect change points effectively in both test cases. These measures are only defined across the length of a target sliding window. As they are unsupervised methods, quadrant and modularity scan are only able to detect the transitions between normal and unhealthy (and vice versa). Regardless, we find that both nonlinear methods perform similarly to the attractor network approach and outperform moving statistics measures when detecting the onset of regime changes. This result is unsurprising as both approaches, attractor networks and RQA, track changes in the vector field in phase space. In the former, this is achieved by evaluating transition probabilities between discretised regions, whereas the latter uses the frequency of recurrences.

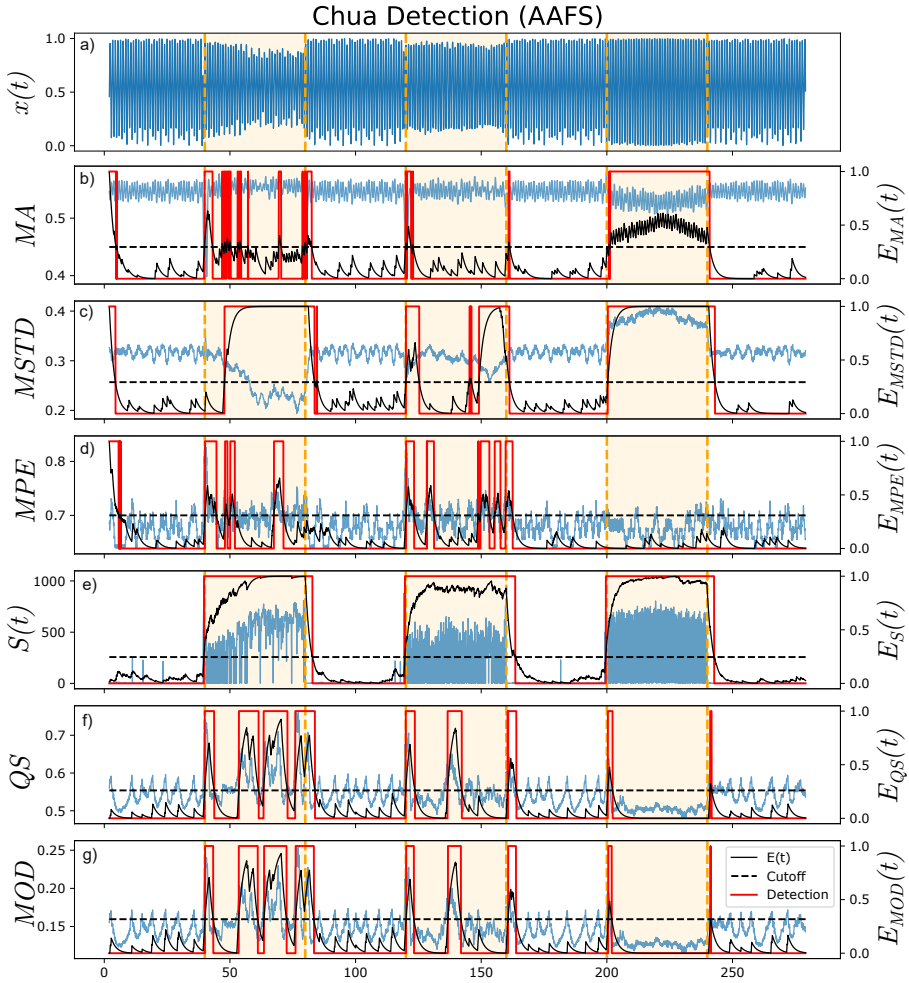
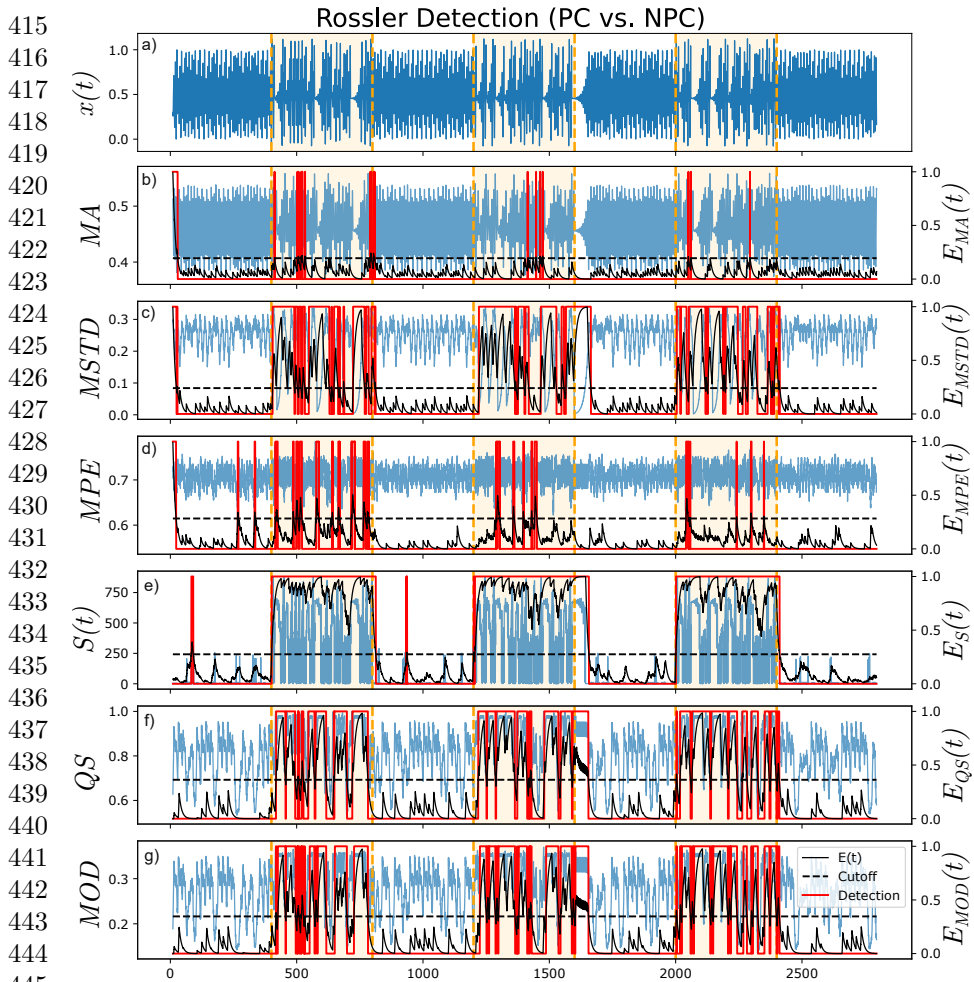


Fig. S8 Change point detection for differentiating between Chua single scroll dynamics and amplitude adjusted Fourier surrogates. Shown: (a) original time series, detection results for (b) moving average, (c) moving standard deviation, (d) permutation entropy, (e) surprise, (f) quadrant scan (QS) and (g) modularity scan (MOD).

References

- [1] Zou, Y., Donner, R.V., Wickramasinghe, M., Kiss, I.Z., Small, M., Kurths, J.: Phase coherence and attractor geometry of chaotic electrochemical oscillators. *Chaos* **22**(3), 033130 (2012)
- [2] Zou, Y., Donner, R.V., Kurths, J.: Geometric and dynamic perspectives on phase-coherent and noncoherent chaos. *Chaos* **22**(1), 013115 (2012)
- [3] Kengne, J.: On the dynamics of Chua's oscillator with a smooth cubic nonlinearity: Occurrence of multiple attractors. *Nonlinear Dynamics* **87**(1), 414



446 **Fig. S9** Change point detection for differentiating between PC and NPC Rössler. Shown:
 447 (a) original time series, detection results for (b) moving average, (c) moving standard deviation,
 448 (d) permutation entropy, (e) surprise, (f) quadrant scan (QS) and (g) modularity scan
 449 (MOD).

450 363–375 (2017)

451

452 [4] Marwan, N., Romano, M.C., Thiel, M., Kurths, J.: Recurrence plots for the
 453 analysis of complex systems. *Physics Reports* **438**(5-6), 237–329 (2007)

454

455 [5] Rapp, P.E., Darmon, D.M., Cellucci, C.J.: Hierarchical transition
 456 chronometries in the human central nervous system. In: *Proceedings from
 457 the International Conference on Nonlinear Theory and Applications* (2013)

458

459 [6] Goswami, B.: A brief introduction to nonlinear time series analysis and
 460 recurrence plots. *Vibration* **2**(4), 332–368 (2019)